Resonance Raman Spectra of a Perylene Bis(dicarboximide) Chromophore in Ground and Lowest Triplet States

ARTICLE *in* THE JOURNAL OF PHYSICAL CHEMISTRY A · SEPTEMBER 2013

Impact Factor: 2.69 · DOI: 10.1021/jp407879k · Source: PubMed

3 AUTHORS, INCLUDING:

Chen Wang
Northwestern University
13 PUBLICATIONS **335** CITATIONS

THE JOURNAL OF PHYSICAL CHEMISTRY A

Article

pubs.acs.org/JPCA

Resonance Raman Spectra of a Perylene Bis(dicarboximide) Chromophore in Ground and Lowest Triplet States

Maria Angelella, Chen Wang, and Michael J. Tauber*

Department of Chemistry and Biochemistry, University of California at San Diego, La Jolla, California 92093, United States

Supporting Information

ABSTRACT: Resonance Raman spectroscopy is employed to probe the ground (S_0) and lowest triplet (T_1) excited states of a perylene bis(dicarboximide) (PDI) dimer. Four bands at ∼1324, 1507, ∼1535, and 1597 cm^{-1} are signatures of the T_1 excited state; a fifth band at ∼1160 cm^{-1} is tentatively assigned. Density functional calculations of an asymmetrically substituted PDI monomer match the experimental bands of the PDI dimer in both S_0 and T_1 states. The match supports a T_1 excited state that is localized on a single PDI moiety of the dimer. The normal modes of the asymmetrically substituted PDI are correlated with ones calculated for the unsubstituted PDI in the D_{2h} point group. Patterns in the Raman intensities are consistent with an A-term mechanism of enhancement. The positions of six bands are predicted for the resonance Raman spectrum of unsubstituted PDI in its T_1 excited state. The spectra and normal-mode analysis reported here are expected to facilitate future studies of singlet fission in PDI crystals or other assemblies.

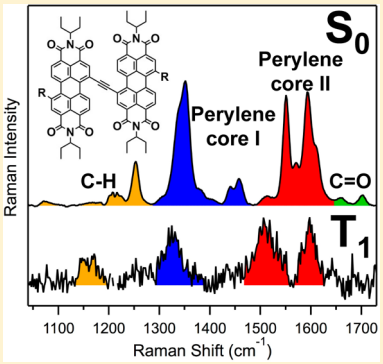

INTRODUCTION

The utilization of triplet excited states in organic molecular photovoltaics is a topic of growing interest.[1−4] Triplet excitons have long (typically microsecond) excited-state lifetimes and therefore exhibit diffusion lengths that are orders of magnitude greater than those of singlet excited states.[4] These advantages could improve the efficiency of various organic photovoltaics (OPVs), such as those based on a bilayer design. The focus on triplet excitons in photovoltaics has sharpened because of a renaissance of research on singlet fission.[5−7] In this mechanism, two triplet excited states form on neighboring molecules from one singlet excited state. A chromophore that is an outstanding candidate for the efficient generation of triplet excitons by fission is perylene bis(dicarboximide) (PDI).[8,9] PDI dyes elicit special interest because they have large absorption cross sections, and are unusually robust and tunable.[10−13] A PDI derivative was incorporated in the first organic molecular photovoltaic,[14] and this family of dyes continues to play an important role in the search for new OPVs.[3,15−17]

In experimental studies, it would be advantageous to utilize a variety of methods for probing triplet excited states of PDI (^{3}PDI*). The first spectroscopic characterization of ^{3}PDI* was by transient absorption (TA) spectroscopy.[18] The $T_1 \rightarrow T_n$ transition in the visible has a cross-section that is only slightly less than that of $S_0 \rightarrow S_1$, and these absorption bands are closely overlapped. Since the pioneering report of Ford and Kamat, TA spectroscopy continues to be a useful probe of ^{3}PDI*.[19−25] Electron paramagnetic resonance (EPR) and optically detected magnetic resonance (ODMR) spectroscopy are powerful techniques for identifying and characterizing triplet states of organic molecules, and their application to ^{3}PDI* has been demonstrated.[26−31] Surprisingly, the vibrational spectroscopy of ^{3}PDI* is largely unexplored. Among the few studies of PDI excited states by vibrational spectroscopy,[32−35] only one has recently identified several IR absorption bands of a triplet excited state.[34] Here, we report resonance Raman spectra of a PDI dimer **1** (Scheme 1) in its ground and lowest triplet states. The spectra of the S_0 and T_1 states of **1** are analyzed by comparison with vibrational normal mode calculations of model compounds, including PDI monomers **2** and **3**.

EXPERIMENTAL SECTION

Dimer **1** was synthesized as described previously.[36] The product was purified by column chromatography with silica 60−200 μm in diameter and a 1:1 (v/v) acetone/methanol eluent. The purity was checked by analysis of ^{1}H NMR spectra of concentrated solutions of **1** in $CDCl_3$, and by absorption and fluorescence spectroscopy. Samples were rinsed with methanol or hexane to reduce grease impurities, if indicated by broad peaks at ∼1.25 and ∼1.68 ppm in the NMR spectrum. The dimer was recrystallized in methanol (Fisher Scientific, HPLC grade) prior to measurement of the reported Raman spectra.

For μs-TA spectroscopy of the triplet excited state, zinc tetraphenylporphyrin (ZnTPP) was used as a triplet sensitizer. A toluene solution of **1** (∼8 μM) and ZnTPP (∼4 μM) was prepared in a glovebox and loaded in a sealed cuvette. The spectra were acquired with a home-built system.[37] The pump wavelength was 431 nm, where the strong Soret transition of ZnTPP accounted for more than ∼80% of the absorbed photons. For steady-state Raman spectroscopy of the triplet

Received: August 7, 2013
Revised: August 22, 2013
Published: September 11, 2013

dx.doi.org/10.1021/jp407879k | J. Phys. Chem. A 2013, 117, 9196−9204

Scheme 1. Experimental PDI Dimer 1; Model PDI Monomers 2,3[a]

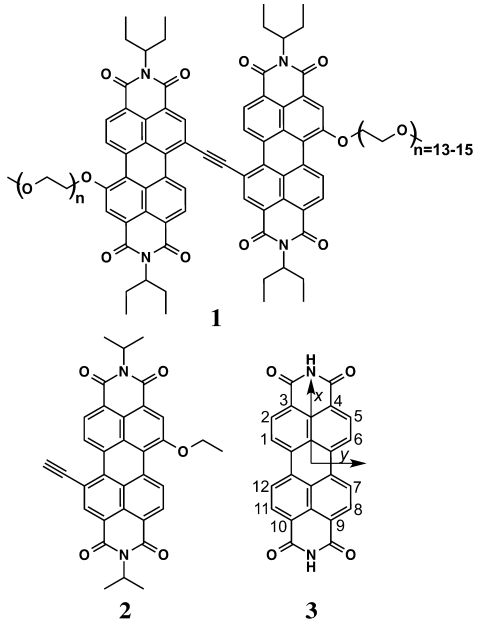

[a]Dimer **1** is the experimental molecule. The polyethylene glycol (PEG) substituents have 13−15 repeat units. Monomers **2** and **3** are two model compounds explored with computations.

excited state, a toluene solution of **1** (~30 μM) with ZnTPP (~14 μM) was prepared in an oxygen-free environment and contained in a sealed cuvette. ZnTPP was photoexcited with 405 nm pulses at 88 MHz (quasi-CW). The Raman probe wavelengths consisted of either a 488.0 or 496.5 nm continuous-wave beam from an argon/krypton ion laser. Spectra were acquired with a 90 degree scattering geometry. The resolution of the spectrograph was ~4 cm^{-1}. Degradation of samples was less than 5% during the course of the experiments, as monitored by UV−vis absorption spectroscopy. The Raman spectrum of the ground state was acquired with a toluene solution of **1**, a probe wavelength of 488.0 nm, and the same detection system as used for the spectroscopy of the triplet excited state.

A new correction procedure was implemented to overcome column-to-column variation in the sensitivity of the CCD. The spectra of **1** benefited from this correction particularly when residual impurities elevated the fluorescence background in the spectral window. In brief, the procedure incorporated the pump-induced emission from the sample as part of the instrument response. Emission from the probed area was more effective than diffuse white light in reducing artifacts caused by the detector. The instrument response spectrum (IRS_{sample}) relates to one typically acquired with a calibrated white light (IRS_{wl}) as follows:

$$IRS_{sample} = \frac{(\text{pump only})}{(\text{pump only})_{smoothed}}(IRS_{wl}) \quad (1)$$

The correction procedure avoids the need for spectral reconstruction from derivative features, as in shifted-excitation Raman difference spectroscopy (SERDS) or subtracted shifted Raman spectroscopy.[38,39] Final spectra reported in Figures 2 and 4 benefited only marginally from the new procedure, because they were acquired with highly purified samples with a low fluorescence background.

Computations were performed with density functional theory (DFT) using Gaussian 09W software.[40] All calculations employed the B3LYP functional and a 6-31G(d) basis set. Frequencies of normal modes and computed spectra were scaled by 0.972. The triplet state computations were obtained by restricting the spin of the molecule. Normal mode diagrams were prepared using Jmol.[41]

Additional description of experiments and computations is provided in the Supporting Information.

RESULTS AND DISCUSSION

Our study focuses on dimer **1** in toluene for two reasons. First, the dimer is soluble and stable in toluene under the conditions of pump−probe and other optical spectroscopy. In general, solubility is important for triplet sensitization. A second reason is that the fluorescence quantum yield of **1** is unusually low (less than 10%) for a solvated PDI molecule.[36] Low fluorescence emission is important for the acquisition of spontaneous Raman spectra with visible excitation.

The visible absorption spectrum of **1** in toluene (Figure 1) differs significantly from that of typical PDI monomers.[13] The

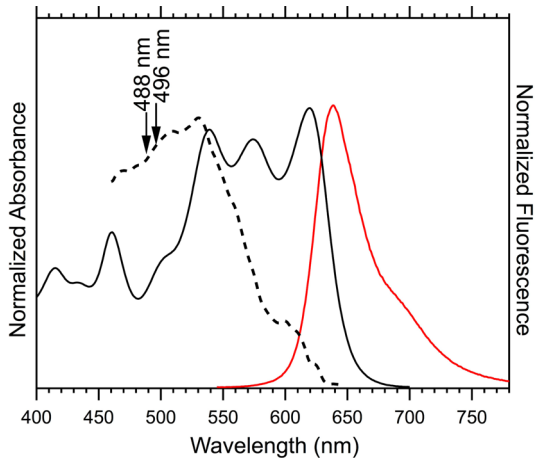

Figure 1. Normalized absorption and emission spectra of **1** in toluene. (Solid black curve) Absorption spectrum of ground state. (Dashed black curve) Absorption spectrum of the triplet excited state, ^{3}**1*** (see SI). Vertical arrows indicate the Raman probe wavelengths. (Red curve) Fluorescence spectrum.

differences are an expected consequence of the electronic communication of two PDI units via the ethyne linker.[36,42] Some characteristics of the absorption and fluorescence spectra of **1** suggest that it may self-assemble in toluene; conversely, other evidence does not support aggregation. Our results lead us to favor an intramolecular explanation for solvent-dependent changes (see SI). However, if aggregation were to occur, it would have little impact on the present work because the wave function of the triplet exciton is expected to be localized (i.e., on a single molecule).[2,43−45]

Resonance Raman Spectroscopy of the Ground (S_0) State of PDI. The experimental resonance Raman spectrum of **1** in toluene is illustrated in Figure 2. The spectrum generally corresponds to published resonance Raman spectra of PDI.[46−48] However, Raman spectra of PDI with substituents attached to the perylene core have not been reported previously. Substituents attached to the bay regions of **1**

dx.doi.org/10.1021/jp407879k | J. Phys. Chem. A 2013, 117, 9196−9204

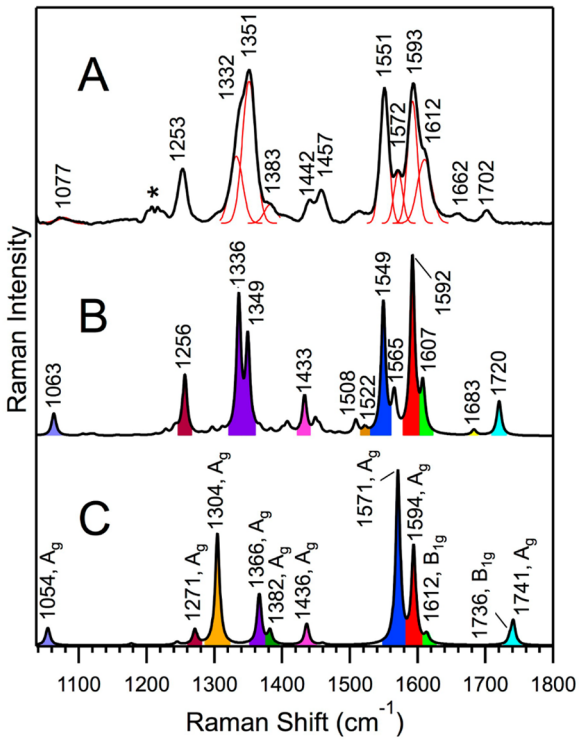

Figure 2. Raman spectrum of dimer **1** in the S_0 state, compared with calculated spectra of model monomers **2** and **3**. (A) Experimental spectrum acquired with 488.0 nm excitation in toluene. Portions of the spectrum are fitted with Gaussian functions (red). An asterisk (*) denotes imperfect subtraction of a Raman band of the solvent. (B) Calculated spectrum of asymmetrically substituted PDI monomer, **2**. (C) Calculated spectrum of PDI monomer with no substituents, **3**. The symmetry of each mode in the D_{2h} point group of **3** is indicated. Calculated spectra have frequencies scaled by a factor of 0.972. The color-coding of bands indicates the correlation of normal modes between model compounds **2** and **3** or between S_0 and T_1 states (Figure 4).

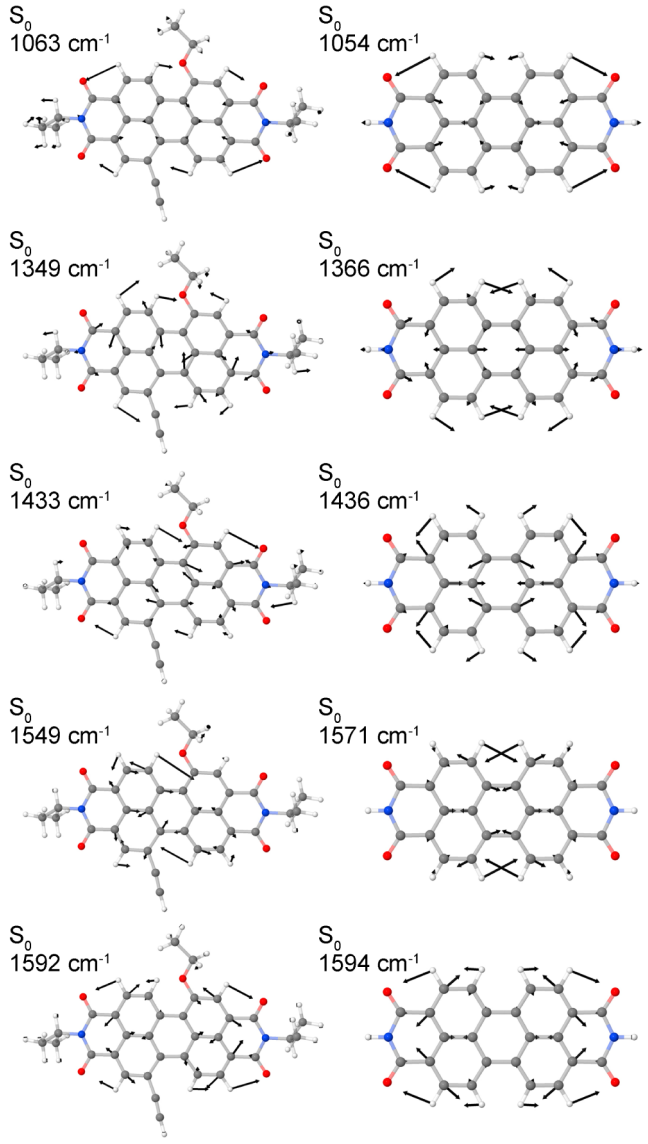

Figure 3. (Left column) Normal modes of model monomer **2** that have a close correspondence in frequency with representative experimental bands of **1** in the S_0 state. (Right column) Normal modes of model monomer **3** in the S_0 state that are the closest match to those of **2**.

lower the local symmetry of each PDI moiety and cause significant changes in the resonance Raman spectrum. The analysis of the experimental spectrum of **1** relies upon DFT/normal mode calculations of three model PDI systems. The calculated off-resonance Raman spectrum of an asymmetric PDI monomer with ethoxy and ethyne substituents attached to its bay positions, **2**, is a good match to the experimental spectrum of **1** in the 1000−1800 cm^{-1} window (Figure 2).

The computed spectrum of a model monomeric PDI without substituents at the bay positions and only H-atoms at the imide groups, **3**, is not as good of a match to experiment. Nonetheless, one can identify normal modes of **3** that have similar frequencies and patterns of vibration, relative to the asymmetrically substituted molecule (Figure 3). Furthermore, molecule **3** has high symmetry (D_{2h} point group), which simplifies its vibrational structure and assists in the understanding of more complex molecules **1** and **2**. The unsubstituted monomer **3** has 114 normal modes, of which 77 are in-plane. A subset of 39 modes has even (*gerade*) symmetry upon inversion, as required for Raman scattering in the D_{2h} point group. Of the 20 vibrational normal modes with A_g symmetry, there are 10 with frequencies in the range 1000−1800 cm^{-1}, 3 are C−H or N−H stretches with higher values, and all remaining modes are less than 1000 cm^{-1}. Of the 19 modes with B_{1g} symmetry, there are 11 with frequencies in the range 1000−1800 cm^{-1}, 2 are C−H stretches with higher values, and all others are less than 1000 cm^{-1}.

Calculations were also performed on a third model compound with two PDI units linked by an ethyne group and two ethoxy substituents at the outer bay positions (**4**, see SI). Despite the similarity of **4** to the experimental dimer, its calculated Raman spectrum does not improve upon that of **2** in matching the experimental spectrum. These results indicate that the asymmetry of each PDI moiety of **1**, rather than the electronic coupling of the two chromophores, has the most significant effect on its Raman scattering.

The vibrational normal modes of PDI molecules **1**−**3** can be divided into four sections within the 1000−1800 cm^{-1} spectral window. In the 1000−1300 cm^{-1} subsection, the normal modes are dominated by CH in-plane bends (equivalently, CH rocks). From the match of frequencies it is expected that the experimental bands of **1** at 1077 and 1253 cm^{-1} are well-described by the calculated normal modes of **2** at 1063 and

dx.doi.org/10.1021/jp407879k | J. Phys. Chem. A 2013, 117, 9196−9204

1256 cm^{-1}, respectively (Figure 2). These modes correlate well with the 1054 and 1271 cm^{-1} modes of **3** (Figure 3 and SI). These two vibrations, like others in the 1000−1300 cm^{-1} range, exhibit relatively small displacements of carbon atoms in the perylene core compared with the prominent CH bending motions. The carbon atoms with the most displacement are the interior ones of PDI, for example, carbons of the central ring or along the centerline of perylene, or those to which the diimide groups are attached (C3, C4, C9, C10). Neighboring carbon atoms tend to move along trajectories that are somewhat parallel; this pattern imparts a breathing or collective characteristic to the motion of these modes.

The 1300−1500 cm^{-1} subsection of the spectrum (denoted here as perylene core I) is generally characterized by modes with diminished C−H rocking and enhanced carbon motion relative to those found in the lower frequency window. The carbon atoms with greatest displacements tend to be interior ones of PDI (described above), and again the motion has a bending/breathing characteristic. The pair of bands centered at 1332 and 1351 cm^{-1} in the experimental spectrum of **1** nearly coincide with calculated bands of **2** at 1336 and 1349 cm^{-1}. Such a correspondence suggests that these normal modes of monomer **2** depict the motions of **1** for this pair of bands. However, the vector displacements for these modes of **2** do not correspond well with those of the unsubstituted monomer **3** at similar frequencies (1304, 1366, and 1382 cm^{-1}). For example, only some aspects of the 1349 cm^{-1} mode of **2** match the 1366 cm^{-1} mode of **3**, as illustrated in Figure 3. The displacement vectors are better matched between substituted and unsubstituted PDIs for modes at 1433 cm^{-1} (**2**) and 1436 cm^{-1} (**3**). The combination of central ring distortion and CH rocks of these modes are expected to characterize the motion for either the 1442 or 1457 cm^{-1} bands of **1**.

The 1500−1620 cm^{-1} subsection, denoted perylene core II, includes modes that have the greatest extent of carbon motion and the least CH in-plane bending. The modes of **2** at 1549, 1592, and 1607 cm^{-1} (Figure 3 and SI), as well as the corresponding ones of **3** at 1571, 1594, and 1612 cm^{-1}, exhibit vectors of neighboring atoms that tend to be antiparallel in an obvious stretching motion. These modes of **2**, including a fourth with frequency 1565 cm^{-1}, are expected to depict the motion associated with experimental bands of **1** at 1551, 1572, 1593, and 1612 cm^{-1}.

In the high-frequency window (1620−1800 cm^{-1}), a pair of weak C═O stretching bands of **1** are centered at 1662 and 1702 cm^{-1}. These bands correspond to ones calculated for **2** at 1683 cm^{-1} (asymmetric stretch) and 1720 cm^{-1} (symmetric stretch) or a pair at 1736 and 1741 cm^{-1} for **3**. The only significant band in the region from ∼1800−2200 cm^{-1} is the ethyne stretch. It is observed at 2178 cm^{-1} in the experimental spectrum, at 2146 cm^{-1} for **2**, and 2200 cm^{-1} for the model dimer **4** (see SI).

Several aspects of the band intensities suggest that the A-term mechanism of resonance enhancement[49] is the most important one for the experimental resonance Raman spectrum of **1**. First, we note that resonance Raman intensities of perylene-based pigments have been previously connected to the magnitude of excited-state displacements of their A_g modes.[50,51] The prior work provides general support for the A-term mechanism as the basis for resonance enhancement in this family of chromophores. Second, we find that the strongest bands of the PDI dimer **1** (e.g., 1551, 1593 cm^{-1}) are correlated with fully symmetric modes of the parent molecule **3**. Although this correlation is not proof of A-term resonance enhancement, it is consistent with that mechanism. Any fully symmetric vibration in the D_{2h} point group of **3** can have an excited state displacement. It is reasonable to expect that an analogous normal mode in a lower point group (e.g., for asymmetrically substituted PDI) will also sustain a displacement upon excitation and contribute to A-term Raman scattering. Third, weaker bands of **1** in the same frequency region (1572, 1612 cm^{-1}) are correlated to modes of **3** that are not fully symmetric. The 1612 cm^{-1} band of the experiment correlates to a calculated mode of **3** with B_{1g} symmetry at the same frequency. A mode of **3** with B_{1g} symmetry is an unlikely candidate for A-term scattering, because a frequency change in the excited state or Duschinsky rotation would be required for that mechanism in the D_{2h} point group. Nonetheless, weak A-term enhancement is possible for an analogous normal mode of **1**, because B_{1g} character in D_{2h} translates to A_g character in the approximately C_{2h} point group of **1**. Along similar lines, the mode at 1572 cm^{-1} in the experiment correlates with the 1565 cm^{-1} mode calculated for **2** (see SI). The overall character of the 1565 cm^{-1} mode strongly suggests *ungerade* symmetry from the standpoint of the perylene core, and closely resembles one calculated at 1584 cm^{-1} for **3** with B_{3u} symmetry. The mode is expected to be IR active but Raman-forbidden in the D_{2h} point group. In short, the lowered symmetry of molecule **1** allows significant scattering from some normal modes that are identified as nontotally symmetric in the D_{2h} point group of the parent molecule **3**. However, the intensities of these bands of **1** are not as strong as those that derive from A_g modes of **3**.

The weak intensity of the carbonyl stretching modes of **1** provides further support for an A-term mechanism of resonance enhancement. The bond order of the C═O groups does not change with the HOMO→LUMO excitation. Therefore one would not expect significant Franck−Condon displacement along modes involving carbonyl stretches.

We note that B-term scattering is another mechanism for enhancement in resonance Raman spectroscopy.[52] The term depends upon vibronic coupling of two excited electronic states that are nearby in energy. As one example, in the model D_{2h} point group, a B_{1g} mode could couple the S_1 state (B_{3u} symmetry with axes selected as in Scheme 1) with any excited state that has B_{2u} symmetry because the direct product $B_{3u} \otimes B_{1g} \otimes B_{2u}$ is fully symmetric. However, modes that transform as B_{1g} in the D_{2h} point group of the parent PDI molecule **3** are totally symmetric in the lower point group of **1**. In short, we find no reason to extend beyond the Albrecht A-term to explain the resonance Raman bands of **1** in its ground state.

One intriguing observation is that the intensity pattern of the experimental spectrum [1253m; (1332m, 1351s); (1551s, 1572m, 1593s, 1612m)] tracks with the calculated intensities of **2** [1256m; (1336s, 1349s); (1549s, 1565m, 1592s, 1607m)] where m and s denote medium- and strong- intensity bands, respectively. The agreement is surprising because the relative intensities of the experimental resonance Raman bands depend upon mode-specific displacements that are not included in the calculations. One qualitative explanation relates to the symmetry arguments described above, where the strongest experimental bands appear to have a close connection with fully symmetric modes in the D_{2h} point group, and less intense bands correlate to modes that are not totally symmetric. Similarly, the calculated Raman intensities (polarizability derivatives) are generally greatest for modes of **2** that correlate with fully symmetric modes of **3** in the parent D_{2h} point group.

dx.doi.org/10.1021/jp407879k | J. Phys. Chem. A 2013, 117, 9196−9204

Although the match of relative band intensities between experiment and computation is good over the 1200−1620 cm^{-1} window, there is less agreement for the carbonyl region, and the ethyne stretch. A quantitative match over the full experimental window would require calculations of the excited state displacement for each mode.

Resonance Raman Spectroscopy of the Triplet Excited State (^{3}PDI*). Raman spectroscopy of the triplet excited state of **1** relied upon the formation of a steady-state population of ^{3}**1***. The sensitizer was ^{3}ZnTPP*. The buildup of ^{3}**1*** population was favored with its long 140 μs lifetime (see SI). The Raman probe wavelengths, 488.0 and 496.5 nm, were selected to be resonant with the strong visible absorption band of ^{3}**1*** (Figure 1). The Raman spectra of the T_1 excited state of **1** are illustrated in Figure 4. Given the low signal-to-noise ratio, a comparison of these two spectra acquired with different wavelengths is a useful check of the reliability of each band. The quality of these T_1 spectra is not as good as the ground-state spectrum, for three reasons. First, the steady-state concentration of the T_1 excited state is only 15−20% that of the ground state. Second, the pump beam causes the background fluorescence in the probe window to approximately double in intensity relative to the probe-only (see SI); therefore, the shot noise is worse by a $\sqrt{2}$. A third factor is revealed upon inspection of the excited-state Raman difference spectra (Figure S8). The amplitudes of the most positive T_1 Raman signals are only a fraction (~1/4) of the most negative S_0 bands. This finding was unexpected, because the probe wavelengths were selected for resonance with the strong $T_1 \rightarrow T_n$ absorption band.

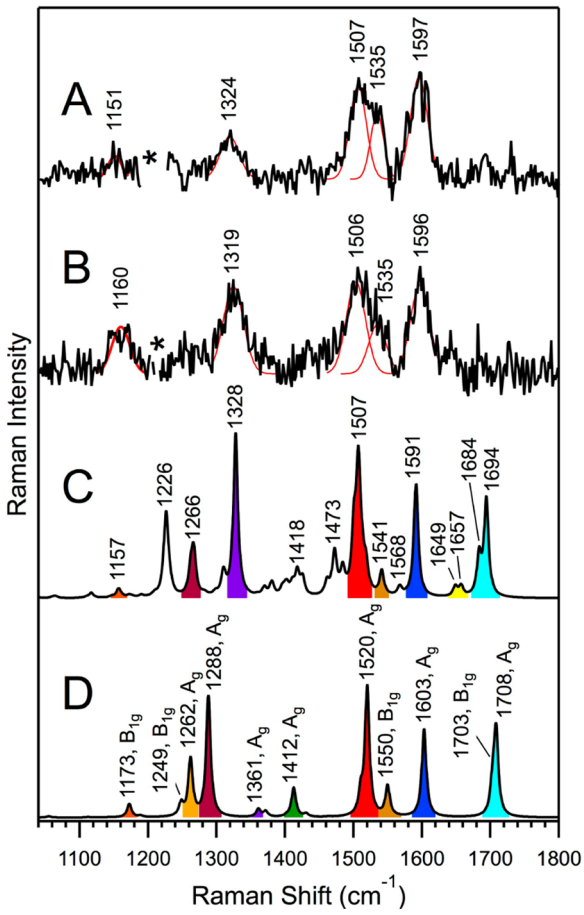

Figure 4. Comparison of Raman spectra of dimer **1** in the T_1 excited state versus calculated spectra of model compounds **2** and **3**. (A) Resonance Raman spectrum of ^{3}**1*** in toluene with 488.0 nm probe. The spectrum is fitted with Gaussian functions (red) and labeled frequencies are their center positions. An asterisk (*) denotes imperfect subtraction of the toluene Raman scattering. (B) Same as A, but with a 496.5 nm probe. (C) Calculated spectrum of asymmetrically substituted PDI monomer, **2**. (D) Calculated spectrum of PDI monomer with no substituents at the bay positions, **3**. The symmetry of each mode in the D_{2h} point group of the PDI core is indicated. Calculated spectra have their frequency axes scaled by a factor of 0.972. Color-coding of bands indicates correlation of normal modes between model compounds **2** and **3** or between T_1 and S_0 states (Figure 2).

Four prominent T_1 bands of **1** are fitted with Gaussian functions centered at ~1324, 1507, ~1535, and 1597 cm^{-1}. A fifth band at ~1160 cm^{-1} is likely, although it is hardly evident in the spectrum with 488.0 nm excitation. Among the calculated bands of the asymmetrically substituted model molecule **2**, five are a good match to the observed experimental bands. This correspondence is important for assigning experimental bands to normal modes of vibration (Figures 4 and 5). Following the analysis of the S_0 state, the modes of the T_1 Raman spectra in the frequency range 1000−1800 cm^{-1} can be partitioned into four subsections: 1000−1300 cm^{-1}, 1300−1500 cm^{-1}, 1500−1620 cm^{-1}, and 1620−1800 cm^{-1}. The 1160 cm^{-1} band in the one experimental spectrum matches a weak band calculated for **2** at 1157 cm^{-1}. The mode of **2** consists primarily of CH in-plane bends, as expected in this subsection. If one overlooks the bay-region substituents, the vectors indicate that the parent mode in the D_{2h} point group has B_{1g} symmetry. A mode of monomer **3** with that symmetry has a frequency of 1173 cm^{-1} (Figure 5). The 1324 cm^{-1} band in the experimental spectrum corresponds to the 1328 cm^{-1} mode of **2** and consists mainly of CH in-plane bends, CC stretches at the bay-region, and central ring-breathing. The displacement vectors suggest that the symmetry of this mode would be A_{1g} in the D_{2h} point group (i.e., if substituents were not considered). The mode of **3** closest in frequency with that symmetry is found at 1361 cm^{-1}, and there is some overlap of vector displacements for molecules **2** and **3**. Next, the 1507 cm^{-1} band in the experiment is a close match to one calculated at identical frequency for **2** and at 1520 cm^{-1} for **3**. The normal mode of **3** is totally symmetric and includes stretches of the CC single bonds of the perylene core, as well as outer diagonal CC bonds (C2C3, C4C5, C8C9, C10C11). The 1535 cm^{-1} band in the experiment probably correlates with the 1541 cm^{-1} mode calculated for **2**, and the 1550 cm^{-1} mode (B_{1g}) for **3**. The dominant motions of both modes are out-of-phase longitudinal stretches of the outer CC bonds of perylene that are parallel to the long axis (C1C2, C5C6, C7C8, C11C12). Finally, the experimental band at ~1597 cm^{-1} is correlated to the 1591 cm^{-1} in-phase longitudinal stretch of **2** and the 1603 cm^{-1} mode (A_{1g}) of **3**. The experimental and calculated modes are summarized in Table 1.

The generalization described above about Raman intensities for the S_0 state appears to hold true for the T_1 state: the strongest resonance enhancements are associated with modes that correlate with fully symmetric ones in the D_{2h} point group. The two bands that are strongest in both spectra (1507, 1597 cm^{-1}), as well as the 1319/1324 cm^{-1} band (third most intense with 496.5 nm excitation), are correlated with A_{1g} modes of the parent D_{2h} point group. The ~1160 cm^{-1} band is weak in the experimental spectra, and it correlates to a mode with B_{1g} symmetry in the D_{2h} point group. Along the same lines, a band

dx.doi.org/10.1021/jp407879k | J. Phys. Chem. A 2013, 117, 9196−9204

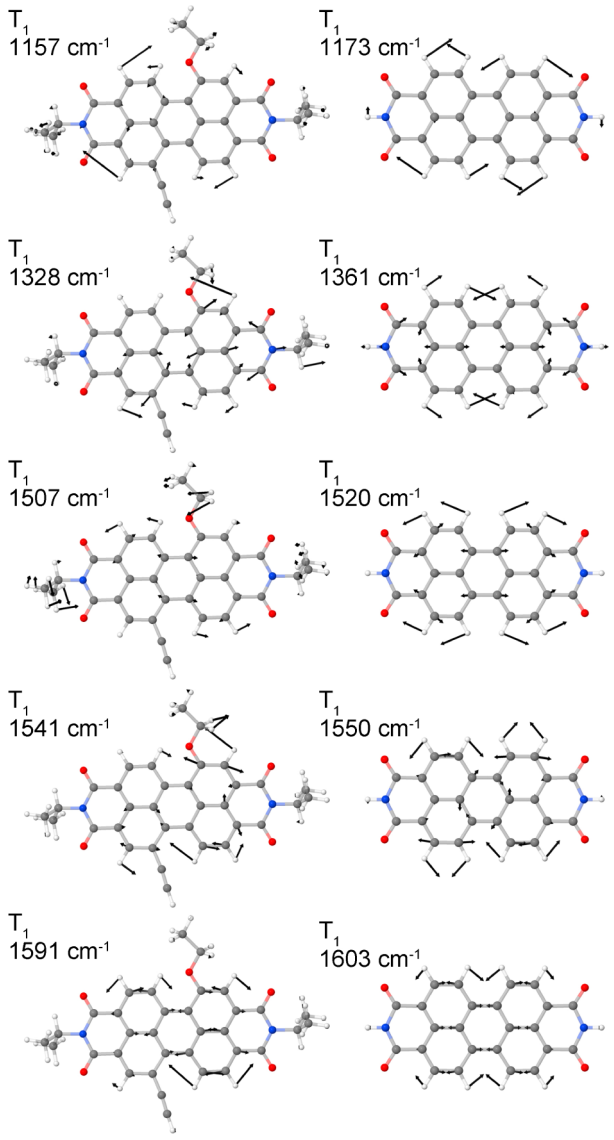

Figure 5. (Left column) Normal modes of the model PDI monomer **2** that have a close correspondence in frequency with experimental bands of **1** in the T_1 excited state. (Right column) Normal modes of model monomer **3** in the T_1 state that are the closest match to those of **2**.

that is predicted in the off-resonance calculations at 1226 cm^{-1} for **2** does not appear above the noise level of the experimental spectra. The vectors of this mode suggest that it would have B_{1g} symmetry in D_{2h}; therefore the excited-state displacement of the equivalent mode in the lower (approximately C_{2h}) point group of **1** is probably insufficient for A-term enhancement. The calculated spectrum also predicts a strong Raman band (CO stretch) at 1694 cm^{-1}, whereas no band in that region is observed in our experimental spectra. Analogous to the $S_0 \rightarrow S_1$ excitation of the ground state, it is likely that the bond order of the carbonyl groups does not change upon $T_1 \rightarrow T_n$ excitation. Therefore a small Franck–Condon displacement is one explanation for the mismatch between the experimental resonance Raman spectrum and the off-resonance calculation.

In the analysis above, we have assumed that the best model system for the T_1 excited state of **1** is an asymmetric monomer, **2**. The use of **2** was suggested by the successful match of its calculated bands in the S_0 state, to the experimental ground-state vibrational spectrum of **1**. However, for the T_1 state, one must consider an additional question that is unrelated to the ground state: How delocalized is the triplet excited-state wave function? The calculated molecular orbitals of **1** imply that the T_1 excited state is distributed equally over both chromophores. The comparison of experimental and simulated Raman spectra of the T_1 state leads to a different conclusion. The spectrum calculated for model dimer **4** is an inferior match to the experimental T_1 spectra of dimer **1**, in comparison with the spectrum of the asymmetric monomer **2** (see SI). The findings based upon experimental Raman bands and the corresponding calculations support the picture of a T_1 excited-state wave function that is localized on a single PDI moiety of dimer **1**, on the femtosecond time scale for resonance Raman scattering.

The localized T_1 state inferred from resonance Raman spectroscopy is also consistent with our results from transient absorption spectroscopy (Figure 1). We note that the $T_1 \rightarrow T_n$ absorption maximum of **1** at ~530 nm is significantly blue-shifted relative to its ground-state absorption band. This blue shift is unlike the more closely matched triplet and ground state absorption bands that have been reported for monomeric PDI.[18,20] The unusual transient spectrum of the dimer could be explained by a T_1 excited-state wave function that is localized on half of the molecule. It is possible that solvent fluctuations cause the loss of symmetry (and collapsed wave function) that is inferred by electronic and vibrational spectroscopy. Triplet

Table 1. Experimental and Computed Raman Frequencies (cm^{-1})

Ground state, S_0			Triplet State, T_1			
1 (expt.)[a]	2 (calc.)[b]	3 (calc.)[b]	1(expt.)[a]	2(calc.)[b]	3(calc.)[b]	Description
1077	1063	1054				
			~1160[c]	1157	1173	Primarily CH rocks
1253	1256	1271		1266	1288	
1332/1351	1336/1349	1366	1324,1319	1328	1361	Perylene core I
1442/1457	1433	1436				
1551	1549	1571	1597	1591	1603	
1572	1565	1584				
1593	1592	1594	1507	1507	1520	Perylene core II
	1522		~1535	1541	1550	
1612	1607	1612				
1662	1683	1736		1649/1657	1703	Carbonyl stretches
1702	1720	1741		1684/1694	1708	
2178	2146			2119		Ethyne stretch

[a]Raman frequencies (cm^{-1}) for **1** or ^{3}**1*** solvated in toluene. [b]DFT calculations for asymmetrically substituted PDI **2** and unsubstituted PDI **3**. [c]Likely band, but not observed with both excitation wavelengths. All implied correlations indicated within each row are best matches for normal modes of model compounds **2** and **3**, or between S_0 and T_1 states. Calculated frequencies are scaled by 0.972.

dx.doi.org/10.1021/jp407879k | J. Phys. Chem. A 2013, 117, 9196–9204

excited states have been found to localize on a single unit in other conjugated systems,[53] including ethyne-linked porphyrin oligomers that are analogous to **1**.[54−56] The fact that triplet excitons are localized in the latter systems on the relatively slow time scale of EPR spectroscopy implies that localization on the faster (fs) time scale of resonance Raman scattering is even more probable.

Comparison of S_0 and T_1 Raman Spectra. Further insights into the nature of the T_1 excited state can be gained by comparison of the normal modes of the T_1 excited state of model molecule **2** with similar modes of the S_0 state. The compilation in Table 1, and the color coding of Figures 2 and 4 aid in this comparison. The relevant normal modes of **2** are pictured in Figures 3 and 5 and the SI. The best match of the 1328 cm^{-1} mode (T_1) is the pair of modes at 1336/1349 cm^{-1} (S_0). The ∼1507 cm^{-1} mode of T_1 is a poor match to nearby S_0 modes at 1508 or 1522 cm^{-1}; however some aspects resemble the 1592 cm^{-1} mode of S_0. The 1541 cm^{-1} mode (T_1) compares well with 1522 cm^{-1} (S_0). The 1591 cm^{-1} mode of T_1 correlates with the 1549 cm^{-1} mode of S_0. Overall, the correspondences between the two states are not straightforward, and the frequency shifts between S_0 and T_1 are not in the same direction for all modes. The reason is that excitation from S_0 to T_1 causes changes in bond orders (see SI for data on HOMO isosurfaces for the two electronic states). These changes result in a normal mode structure in the T_1 excited state that is mixed relative to the ground state (Duschinsky rotation).[57] In the T_1 excited state, the bonds that lengthen 0.03−0.04 Å are the outer diagonal CC bonds (C2C3, C4C5, C8C9, and C10C11) and the four CC bonds in the interior bay region. Their force constants are expected to decrease. Consistent with that change, modes that involve a significant proportion of the outer diagonal or bay region CC bonds are lower in frequency for the T_1 state of **2** versus S_0 (e.g., 1507 cm^{-1} of T_1 versus 1592 cm^{-1} of S_0). In contrast, bonds that shorten by 0.03−0.04 Å upon excitation to the T_1 excited state are C1C2, C5C6, C7C8, and C11C12, and the pair of C−C single bonds that hold the naphthalene units together. Normal modes of **2** that consist primarily of stretches of the shortened bonds should be higher in frequency for the T_1 state, for example, the 1591 cm^{-1} mode for the T_1 state of **2**, versus the 1549 cm^{-1} of its S_0 state.

CONCLUSIONS

In the above sections we have described and analyzed the first Raman spectrum of a triplet exciton in the PDI family. We conclude with three points.

First, the bands of the T_1 excited state are distinguishable from those of the ground (S_0) state. The bands of the T_1 state are also distinguishable from spontaneous resonance Raman or femtosecond-stimulated Raman spectra of PDI anions[33,58] or PDI in its lowest singlet (S_1) excited state.[32,33] The use of different excitation wavelengths in resonance Raman spectroscopy can provide an additional level of selective identification, apart from unique bands for each state. For example, with 1064 nm excitation, signatures from PDI anions are amplified relative to those of the neutral species.[58] Similarly, with visible excitation near ∼500 nm, the signals of ^{3}PDI* state are expected to be significantly enhanced over other species, such as the S_1 excited state (^{1}PDI*) or the ground-state anion (PDI^-).

Second, it is useful to generalize the results here for an experimental dimer and predict key resonance Raman bands for a triplet state (T_1) PDI monomer without substituents attached to the bay region. The three most prominent bands in our experimental spectrum of **1** in the T_1 state (∼1324, 1507, and 1597 cm^{-1}) match those computed for the asymmetric monomer **2** (1328, 1507, and 1591 cm^{-1}). These three vibrational modes of PDI **2** resemble totally symmetric (A_g) modes calculated for unsubstituted PDI **3** at 1361, 1520, and 1603 cm^{-1}, respectively. Therefore, we predict that the triplet excited state of PDI without bay substituents will have resonance Raman bands centered near 1361, 1520, and 1603 cm^{-1}. Additional bands are likely at 1262, 1288, and 1412 cm^{-1}, based upon calculations of A_g normal modes with those frequencies for **3** in the T_1 state.

Third, we note that singlet fission is an expected mechanism for generating triplet excitons of PDI chromophores, if they are packed appropriately.[8,9] Given that the chromophore is generally much less fluorescent when crystalline or aggregated than when solvated,[10] resonance Raman spectroscopy would be well-suited for these studies. An optical arrangement for measuring backscattered light would be ideal for opaque solid samples.

In short, resonance Raman spectroscopy is capable of specifically identifying the T_1 excited state of PDI. The technique could play a significant role in probing solid samples where singlet fission is expected. The comparative analysis of S_0 and T_1 states described in the present work can facilitate such studies.

ASSOCIATED CONTENT

Supporting Information

Additional figures, steady-state state model, resonance Raman data workup, and diagrams of vibrational normal modes. This material is available free of charge via the Internet at http://pubs.acs.org.

AUTHOR INFORMATION

Corresponding Author

*E-mail: mtauber@ucsd.edu.

Notes

The authors declare no competing financial interest.

ACKNOWLEDGMENTS

This work was partially supported by the National Science Foundation under CHE-1057198, the ACS-Petroleum Research Fund, and the Hellman Family Foundation. We thank Jonathan Baram and Boris Rybtchinski (Weizmann Institute of Science) for providing PDI dimer **1**. The contributions of Brendan Connors, Steven Shimizu, Brian Leigh, Rick Thomas, and Hannah Shafaat are much appreciated. The following facilities at UCSD contributed to the research: the Molecular Mass Spectrometry Facility (Yongxuan Su), the Chemistry NMR Facility (Anthony Mrse), and the Physics Electronics Shop. Lastly, we appreciate helpful discussions with Judy Kim (UCSD) and Douglas Magde (UCSD).

REFERENCES

(1) Shao, Y.; Yang, Y. Efficient Organic Heterojunction Photovoltaic Cells Based on Triplet Materials. *Adv. Mater.* **2005**, *17*, 2841−2844.

(2) Köhler, A.; Bässler, H. Triplet States in Organic Semiconductors. *Mater. Sci. Eng. R* **2009**, *66*, 71−109.

(3) Jadhav, P. J.; Brown, P. R.; Thompson, N.; Wunsch, B.; Mohanty, A.; Yost, S. R.; Hontz, E.; Voorhis, T. V.; Bawendi, M. G.; Bulović, V.;

Baldo, M. A. Triplet Exciton Dissociation in Singlet Exciton Fission Photovoltaics. *Adv. Mater.* **2012**, *24*, 6169−6174.
(4) Yost, S. R.; Hontz, E.; Yeganeh, S.; Voorhis, T. V. Triplet vs Singlet Energy Transfer in Organic Semiconductors: The Tortoise and the Hare. *J. Phys. Chem. C* **2012**, *116*, 17369−17377.
(5) Smith, M. B.; Michl, J. Singlet Fission. *Chem. Rev.* **2010**, *110*, 6891−6936.
(6) Smith, M. B.; Michl, J. Recent Advances in Singlet Fission. *Annu. Rev. Phys. Chem.* **2013**, *64*, 361−386.
(7) Burdett, J. J.; Bardeen, C. J. The Dynamics of Singlet Fission in Crystalline Tetracene and Covalent Analogs. *Acc. Chem. Res.* **2013**, *46* (6), 1312−1320.
(8) Paci, I.; Johnson, J. C.; Chen, X.; Rana, G.; Popovic, D.; David, D. E.; Nozik, A. J.; Ratner, M. A.; Michl, J. Singlet Fission for Dye-Sensitized Solar Cells: Can a Suitable Sensitizer be Found? *J. Am. Chem. Soc.* **2006**, *128*, 16546−16553.
(9) Renaud, N.; Sherratt, P. A.; Ratner, M. A. Mapping the Relation between Stacking Geometries and Singlet Fission Yield in a Class of Organic Crystals. *J. Phys. Chem. Lett.* **2013**, *4*, 1065−1069.
(10) Würthner, F. Perylene Bisimide Dyes as Versatile Building Blocks for Functional Supramolecular Architectures. *Chem. Commun.* **2004**, 1564−1579.
(11) Langhals, H. Control of the Interactions in Multichromophores: Novel Concepts. Perylene Bis-imides as Components for Larger Functional Units. *Helv. Chim. Acta* **2005**, *88*, 1309−1343.
(12) Herrmann, A.; Müllen, K. From Industrial Colorants to Single Photon Sources and Biolabels: The Fascination and Function of Rylene Dyes. *Chem. Lett.* **2006**, *35* (9), 978−985.
(13) Huang, C.; Barlow, S.; Marder, S. R. Perylene-3,4,9,10-tetracarboxylic Acid Diimides: Synthesis, Physical Properties, and Use in Organic Electronics. *J. Org. Chem.* **2011**, *76*, 2386−2407.
(14) Tang, C. W. Two-layer Organic Photovoltaic Cell. *Appl. Phys. Lett.* **1986**, *48* (2), 183−185.
(15) Howard, I. A.; Laquai, F.; Keivanidis, P. E.; Friend, R. H.; Greenham, N. C. Perylene Tetracarboxydiimide as an Electron Acceptor in Organic Solar Cells: A Study of Charge Generation and Recombination. *J. Phys. Chem. C* **2009**, *113*, 21225−21232.
(16) Ramanan, C.; Smeigh, A. L.; Anthony, J. E.; Marks, T. J.; Wasielewski, M. R. Competition between Singlet Fission and Charge Separation in Solution-Processed Blend Films of 6,13-Bis-(triisopropylsilylethynyl)-pentacene with Sterically-Encumbered Perylene-3,4:9,10-bis(dicarboximide)s. *J. Am. Chem. Soc.* **2012**, *134*, 386−397.
(17) Li, C.; Wonneberger, H. Perylene Imides for Organic Photovoltaics: Yesterday, Today, and Tomorrow. *Adv. Mater.* **2012**, *24*, 613−636.
(18) Ford, W. E.; Kamat, P. V. Photochemistry of 3,4,9,10-Perylenetetracarboxylic Dianhydride Dyes. 3. Singlet and Triplet Excited-State Properties of the Bis(2,5-di-tert-butylphenyl)imide Derivative. *J. Phys. Chem.* **1987**, *91*, 6373−6380.
(19) Sadrai, M.; Hadel, L.; Sauers, R. R.; Husain, S.; Krogh-Jespersen, K.; Westbrook, J. D.; Bird, G. R. Lasing Action In a Family of Perylene Derivatives: Singlet Absorption and Emission Spectra, Triplet Absorption and Oxygen Quenching Constants, and Molecular Mechanics and Semiempirical Molecular Orbital Calculations. *J. Phys. Chem.* **1992**, *96* (20), 7988−7996.
(20) Kircher, T.; Löhmannsröben, H. G. Photoinduced Charge Recombination Reactions of a Perylene Dye in Acetonitrile. *Phys. Chem. Chem. Phys.* **1999**, *1*, 3987−3992.
(21) Rachford, A. A.; Goeb, S.; Castellano, F. N. Accessing the Triplet Excited State of Perylenediimides. *J. Am. Chem. Soc.* **2008**, *130*, 2766−2767.
(22) Danilov, E. O.; Rachford, A. A.; Goeb, S.; Castellano, F. N. Evolution of the Triplet Excited State in Pt(II) Perylenediimides. *J. Phys. Chem. A* **2009**, *113*, 5763−5768.
(23) Veldman, D.; Chopin, S. M. A.; Meskers, S. C. J.; Groeneveld, M. M.; Williams, R. M.; Janssen, R. A. J. Triplet Formation Involving a Polar Transition State in a Well-Defined Intramolecular Perylenediimide Dimeric Aggregate. *J. Phys. Chem. A* **2008**, *112*, 5846−5857.
(24) Hofmann, C. C.; Lindner, S. M.; Ruppert, M.; Hirsch, A.; Haque, S. A.; Thelakkat, M.; Köhler, J. Mutual Interplay of Light Harvesting and Triplet Sensitizing in a Perylene Bisimide Antenna-Fullerene Dyad. *J. Phys. Chem. B* **2010**, *114*, 9148−9156.
(25) Flamigni, L.; Zanelli, A.; Langhals, H.; Böck, B. Photophysical and Redox Properties of Perylene Bis- and Tris-Dicarboximide Fluorophores with Triplet State Formation: Transient Absorption and Singlet Oxygen Sensitization. *J. Phys. Chem. A* **2012**, *116*, 1503−1509.
(26) Dance, Z. E. X.; Mi, Q.; McCamant, D. W.; Ahrens, M. J.; Ratner, M. A.; Wasielewski, M. R. Time-Resolved EPR Studies of Photogenerated Radical Ion Pairs Separated by *p*-Phenylene Oligomers and of Triplet States Resulting from Charge Recombination. *J. Phys. Chem. B* **2006**, *110*, 25163−25173.
(27) Carmieli, R.; Zeidan, T. A.; Kelley, R. F.; Mi, Q.; Lewis, F. D.; Wasielewski, M. R. Excited State, Charge Transfer, and Spin Dynamics in DNA Hairpin Conjugates with Perylenediimide Hairpin Linkers. *J. Phys. Chem. A* **2009**, *113*, 4691−4700.
(28) Miura, T.; Carmieli, R.; Wasielewski, M. R. Time-Resolved EPR Studies of Charge Recombination and Triplet-State Formation within Donor-Bridge-Acceptor Molecules Having Wire-Like Oligofluorene Bridges. *J. Phys. Chem. A* **2010**, *114*, 5769−5778.
(29) Colvin, M. T.; Giacobbe, E. M.; Cohen, B.; Miura, T.; Scott, A. M.; Wasielewski, M. R. Competitive Electron Transfer and Enhanced Intersystem Crossing in Photoexcited Covalent TEMPO-Perylene-3,4:9,10-bis(dicarboximide) Dyads: Unusual Spin Polarization Resulting from the Radical-Triplet Interaction. *J. Phys. Chem. A* **2010**, *114*, 1741−1748.
(30) Lifshitz, E.; Kaplan, A.; Ehrenfreund, E.; Meissner, D. Magneto-optical Studies of Perylene Tetracarboxylic Acid Diimide Thin Films. *Opt. Mater.* **1998**, *9*, 295−298.
(31) Lifshitz, E.; Kaplan, A.; Ehrenfreund, E.; Meissner, D. Optically Detected Magnetic Resonance as a Tool to Study the Morphology of Perylene-Derivative Thin Film. *Chem. Phys. Lett.* **1999**, *300*, 626−632.
(32) Mier, L.; Min, Y.; Danilov, E. O.; Epstein, A. J.; Gustafson, T. L., Ultrafast Vibrational Spectroscopy of Perylene Diimide Complexes. In *XXII International Conference on Raman Spectroscopy*; American Institute of Physics: College Park, MD, 2010.
(33) Brown, K. E.; Veldkamp, B. S.; Co, D. T.; Wasielewski, M. R. Vibrational Dynamics of a Perylene-Perylenediimide Donor-Acceptor Dyad Probed with Femtosecond Stimulated Raman Spectroscopy. *J. Phys. Chem. Lett.* **2012**, *3*, 2362−2366.
(34) Prusakova, V.; McCusker, C. E.; Castellano, F. N. Ligand-Localized Triplet-State Photophysics in a Platinum(II) Terpyridyl Perylenediimideacetylide. *Inorg. Chem.* **2012**, *51*, 8589−8598.
(35) Alberding, B. G.; Brown-Xu, S. E.; Chisholm, M. H.; Epstein, A. J.; Gustafson, T. L.; Lewis, S. A.; Min, Y. Photoinduced Charge Transfer Involving a MoMo Quadruply Bonded Complex to a Perylene Diimide. *Dalton Trans.* **2013**, *42*, 5275−5280.
(36) Baram, J.; Shirman, E.; Ben-Shitrit, N.; Ustinov, A.; Weissman, H.; Pinkas, I.; Wolf, S. G.; Rybtchinski, B. Control Over Self-Assembly through Reversible Charging of the Aromatic Building Blocks in Photofunctional Supramolecular Fibers. *J. Am. Chem. Soc.* **2008**, *130*, 14966−14967.
(37) Wang, C.; Angelella, M.; Kuo, C.-H.; Tauber, M. J. Singlet Fission in Carotenoid Aggregates: Insights from Transient Absorption Spectroscopy. *Proc. SPIE* **2012**, 8459.
(38) Shreve, A. P.; Cherepy, N. J.; Mathies, R. A. Effective Rejection of Fluorescence Interference in Raman Spectroscopy Using a Shifted Excitation Difference Technique. *Appl. Spectrosc.* **1992**, *46* (4), 707−711.
(39) Bell, S. E. J.; Bourguignon, E. S. O.; Dennis, A. Analysis of Luminescent Samples Using Subtracted Shifted Raman Spectroscopy. *Analyst* **1998**, *123*, 1729−1734.
(40) Frisch, M. J.; Trucks, G. W.; Schlegel, H. B.; Scuseria, G. E.; Robb, M. A.; Cheeseman, J. R.; Scalmani, G.; Barone, V.; Mennucci, B.; Petersson, G. A.; et al. *Gaussian 09*; Gaussian Inc.: Wallingford, CT, 2009.

(41) *Jmol: an open-source Java viewer for chemical structures in 3D*. http://www.jmol.org/
(42) Yan, Q.; Zhao, D. Conjugated Dimeric and Trimeric Perylenediimide Oligomers. *Org. Lett.* **2009**, *11* (15), 3426−3429.
(43) Schwoerer, M.; Wolf, H. C. *Organic Molecular Solids*; Wiley-VCH: Weinheim, Germany, 2007.
(44) Tiago, M. L.; Northrup, J. E.; Louie, S. G. Ab initio Calculation of the Electronic and Optical Properties of Solid Pentacene. *Phys. Rev. B* **2003**, *67*, 115212.
(45) Cudazzo, P.; Gatti, M.; Rubio, A. Excitons in Molecular Crystals from First-Principles Many-Body Peturbation Theory: Picene Versus Pentacene. *Phys. Rev. B* **2012**, *86*, 195307.
(46) Akers, K.; Aroca, R.; Hor, A. M.; Loutfy, R. O. Molecular Organization in Perylene Tetracarboxylic Di-imide Solid Films. *Spectrochim. Acta* **1988**, *44A* (11), 1129−1135.
(47) Johnson, E.; Aroca, R.; Nagao, Y. Electronic and Vibrational Spectra of Films and Langmuir-Blodgett Monolayers of N-Octyl-3,4-perylenedicarboximide. *J. Phys. Chem.* **1991**, *95*, 8840−8843.
(48) Zahn, D. R. T.; Gavrila, G. N.; Salvan, G. Electronic and Vibrational Spectroscopies Applied to Organic/Inorganic Interfaces. *Chem. Rev.* **2007**, *107*, 1161−1232.
(49) Myers, A. B.; Mathies, R. A., Resonance Raman Intensities: A Probe of Excited-state Structure and Dynamics. In *Biological Applications of Raman Spectroscopy*; John Wiley & Sons: New York, 1987; Vol. *2*, pp 1−58.
(50) Scholz, R.; Kobitski, A. Y.; Kampen, T. U.; Schreiber, M.; Zahn, D. R. T.; Jungnickel, G.; Elstner, M.; Sternberg, M.; Fraunheim, T. Resonant Raman Spectroscopy of 3,4,9,10-perylene-tetracarboxylic-dianhydride Epitaxial Films. *Phys. Rev. B* **2000**, *61* (20), 13659−13669.
(51) Gisslén, L.; Scholz, R. Crystallochromy of Perylene Pigments: Interference Between Frenkel Excitons and Charge-transfer States. *Phys. Rev. B* **2009**, *80*, 115309.
(52) Albrecht, A. C. On the Theory of Raman Intensities. *J. Chem. Phys.* **1961**, *34* (5), 1476−1484.
(53) Nayyar, I. H.; Batista, E. R.; Tretiak, S.; Saxena, A.; Smith, D. L.; Martin, R. L. Role of Geometric Distortion and Polarization in Localizing Electronic Excitations in Conjugated Polymers. *J. Chem. Theory Comput.* **2013**, *9*, 1144−1154.
(54) Angiolillo, P. J.; Susumu, K.; Uyedo, H. T.; Lin, V. S.-Y.; Shediac, R.; Therien, M. J. Trends in Triplet Excitation Delocalization in Highly Conjugated (Porphinato)zinc(II) Arrays Probed by EPR Spectroscopy. *Synth. Met.* **2001**, *116*, 247−253.
(55) Angiolillo, P. J.; Lin, V. S.-Y.; Vanderkooi, J. M.; Therien, M. J. EPR Spectroscopy and Photophysics of the Lowest Photoactivated Triplet State of a Series of Highly Conjugated (Porphinato)Zn Arrays. *J. Am. Chem. Soc.* **1995**, *117*, 12514−12527.
(56) Angiolillo, P. J.; Uyeda, H. T.; Duncan, T. V.; Therien, M. J. Impact of Electronic Asymmetry on Photoexcited Triplet-State Spin Distributions in Conjugated Porphyrin Oligomers Probed via EPR Spectroscopy. *J. Phys. Chem. B* **2004**, *108*, 11893−11903.
(57) Sando, G. M.; Spears, K. G.; Hupp, J. T.; Ruhoff, T. P. Large Electron Transfer Rate Effects from the Duschinsky Mixing of Vibrations. *J. Phys. Chem. A* **2001**, *105*, 5317−5325.
(58) Gawrys, P.; Louarn, G.; Zagorska, M.; Pron, A. Solid State Electrochemistry and Spectroelectrochemistry of Poly (arylene bisimide-alt-oligoether)s. *Electrochim. Acta* **2011**, *56*, 3429−3435.